Toward Dynamically Adapting Wireless Intra-Chip Channels to Traffic Needs with a Programmable Metasurface

Mohammadreza F Imani, Sergi Abadal, Philipp del Hougne

Toward Dynamically Adapting Wireless Intra-Chip Channels to Traffic Needs with a Programmable Metasurface

Mohammadreza F. Imani
ECEE, Arizona State University
Tempe, AZ, USA
mohammadreza.imani@asu.edu

Sergi Abadal
N3Cat, Univ. Politècnica de Catalunya
Barcelona, Spain
abadal@ac.upc.edu

Philipp del Hougne*
IETR, Univ. Rennes 1
Rennes, France
philipp.delhougne@gmail.com

ABSTRACT

We introduce the idea of endowing on-chip wireless propagation environments with in-situ programmability by equipping the chip package with a programmable metasurface. The limitations of current wired chip interconnect fabrics present a serious performance bottleneck for multi-core chips. Wireless links between far-apart cores are a promising complementary link technique but struggle with the complex on-chip propagation environment presenting strong multipath effects. We expect that these challenges can be addressed with the ability to shape wireless channels between far-apart cores and to dynamically adapt them to traffic needs; for instance, by tailoring the impulse response between two wireless nodes, it may be feasible to prevent inter-symbol interference. Here, we present our recent progress toward this goal, including an analysis of the on-chip propagation environment, an efficient design of programmable meta-atoms suitable for the on-chip environment and operating in the 60 GHz regime, and a detailed discussion of different single-channel and multi-channel use-case scenarios.

CCS CONCEPTS

• **Hardware → Network on chip**; **Emerging technologies**.

KEYWORDS

Wireless Intra-Chip Communication, Wireless Network-on-Chip, Multiprocessor Interconnection, MIMO, Programmable Metasurface, Reconfigurable Intelligent Surface

ACM Reference Format:
Mohammadreza F. Imani, Sergi Abadal, and Philipp del Hougne. 2020. Toward Dynamically Adapting Wireless Intra-Chip Channels to Traffic Needs with a Programmable Metasurface. In *The 1st ACM International Workshop on Nanoscale Computing, Communication, and Applications (NanoCoCoA '20), November 16, 2020, Virtual Event, Japan.* ACM, New York, NY, USA, 6 pages. https://doi.org/10.1145/3416006.3431274

*Author to whom correspondance should be addressed.

NanoCoCoA '20, November 16, 2020, Virtual Event, Japan

ACM ISBN 978-1-4503-8116-1/20/11…$15.00
https://doi.org/10.1145/3416006.3431274

1 INTRODUCTION

The unceasing quest for faster computing has given rise to multi-core processors which integrate multiple processor cores within the same chip. As the number of cores per chip increases, computation speeds increasingly depend not only on the performance of individual cores; instead, on-chip communication [4] between cores to exchange and share data becomes a serious speed bottleneck. Conventional wired interconnects must be kept short which implies an exponentially increasing need for inter-router hops as the number of cores increases. The resulting latency in communication between far-apart cores (up to several tens of nanoseconds [36]) motivates the search for complementary alternative intra-chip links, including ideas such as optical [25] or radiofrequency [5, 24] interconnects. The latter benefit from the availability of mature technology for on-chip antennas and integrated transceivers [17, 28, 39, 40].

Wireless intra-chip links avoid the need for inter-router hops and potentially offer significantly faster communication between far-apart cores. The propagation environment of the wireless signals, however, is confined and highly complex due to multiple material interfaces and the chip package which constitutes an electrically large metallic enclosure. In contrast to free space, such a complex propagation environment gives rise to strong multipath effects, dispersion and attenuation [23]. For the design process of a Wireless Network-on-Chip (WNoC) it is crucial to take these characteristics into account, be it to counteract or to harness the consequences of this complexity. Indeed, coherent wave propagation through non-trivial media is not necessarily an obstacle for information transfer: around the turn of the millennium, it was realised that multiple scattering can in fact increase the achievable capacity because it helps to make different channels more distinguishable [26, 32].

Recently, a new paradigm is emerging in the area of indoor wireless communication: the use of programmable metasurfaces [6] as "reconfigurable intelligent surfaces" (RIS) in order to tweak the propagation environment [13]. A programmable metasurface, also referred to as "tunable impedance surface" [31] or "spatial microwave modulator" [14], is an array of individually programmable meta-atoms with at least two digitalized states with distinct electromagnetic responses. By judiciously programming the states of the individual meta-atoms, the scattering properties of the propagation environment, and thereby the wireless communication channels, can be tuned. While previously the channels were considered fixed and the focus was on engineering the hardware of the transceivers and the software behind the signals, the RIS paradigm now enables the physical shaping of channels for a specific purpose. For instance, recent experimental work demonstrated that the distinguishability of multiple indoor channels can be pushed to its optimum value by tweaking the environment's disorder with a RIS [8]. Moreover,

novel RIS-based backscatter-communication schemes with unique speed and/or security features were prototyped [15, 42]. But the use of programmable metasurfaces in indoor environments is not restricted to shaping communication channels, they can also prove useful for auxiliary tasks like position sensing [10] or gesture recognition [9, 21].

In this project, we seek to transpose the concept of programming the propagation environment to enhance wireless communication from the indoor scale to the on-chip scale. A unique feature of on-chip environments is their static nature – in contrast to indoor environments that constantly evolve due to moving inhabitants, furniture, etc. Recent work already recognized the potential of this quasi-deterministic nature in combination with optimized properties of the system's monolithic nature [35]. Here, we seek to transition from a static on-chip propagation environment to a dynamically adaptable system whose properties can be adjusted in real-time to optimally meet traffic needs. In this paper, we outline our recent progress toward this goal. We begin by characterizing a typical on-chip propagation environment. Next, we outline the design of a programmable meta-atom suitable for the on-chip environment in the targeted 60 GHz range. Finally, we discuss several methods to enhance both single-channel or multi-channel on-chip wireless communication in a programmable environment.

2 CHARACTERIZATION OF ON-CHIP PROPAGATION ENVIRONMENT

We begin our analysis by describing a typical chip and analyzing its physical landscape from the perspective of wave propagation in complex media. Both spatial constraints on the antenna size and the need for high-speed reliable wireless communication point toward operating at higher frequencies in a WNoC than in typical indoor wireless communication. A common choice that we adopt in the following is the millimeter wave (mmW) regime around 60 GHz (free-space wavelength 5 mm).

For concreteness, we consider a single 33 mm × 33 mm package containing a 22 mm × 22 mm chip as illustrated in Fig. 1(a). The chip consists of a 4 × 4 array of cores that is surrounded by air; we neglect that cores are typically interleaved with memory modules in our sketch because this detail is irrelevant for the demonstration of our concept. The package boundaries are metallic (i.e., approximately perfect electric conductors). The chip itself consists of a 0.0875 mm thin layer of solder bumps on top of the package substrate, followed by a 0.011 mm thick silicon-dioxide (SiO_2) layer, a 0.3 mm thick silicon (Si) substrate layer and finally a 0.8 mm thick aluminium nitride (AlN) layer. The billions of transistors performing the computing are located at the interface between SiO_2 and Si layers. Countless metal lines run through the SiO_2 layer to connect the transistors. The AlN layer acts as heat spreader to help with the dissipation of thermal energy. All 16 processors are implemented on one continuous SiO_2-Si interface, i.e. there are no physical gaps between different cores. Dipole or patch antennas can be oriented horizontally within the SiO_2 layer [17, 19, 28]. Alternatively, vertical monopole antennas that pierce through the silicon, so-called "through-silicon vias", can be realized [27, 38].

We envision that the array of programmable meta-atoms will be attached to the inside upper boundary of the package. The meta-atoms can be manufactured separately and integrated after the deposition or growth of the AlN layer using a face-to-face approach. Delivering the bias voltages to the meta-atoms can be envisaged to take place with strategically located through-silicon vias and a distribution network within the metasurface. The existence of meta-atoms and additional circuitry may impact on the heat dissipation capacity of the chip and needs to be further assessed. Each meta-atom can be programmed individually into different states and each state corresponds to a distinct scattering response, as detailed in Section 3. The wave field inside an enclosure like the chip package is the superposition of the field radiated by the source and all the reflections off the material interfaces and boundaries (secondary sources) [1, 23]. If the geometry of the enclosure is irregular, the wave field will be speckle-like. While solely the presence of refraction at material interfaces and reverberation within the enclosure shown in Fig. 1(a) may not result in a fully randomized wave field, the addition of an array of programmable meta-atoms with an irregular pattern of programmed reflection properties to the top boundary of the package certainly will [16]. In a typical speckle-like wave field, the spatial coherence length Δl_{corr} is on the order of $\lambda/2$ and its spectral coherence length depends on its quality factor: $\Delta f_{\text{corr}} = f_0/Q$. This means that the field at two positions separated by more than Δl_{corr} or two frequencies separated by more than Δf_{corr} does not present significant correlations. Within a given frequency band Δf, the number of approximately independent frequencies, termed the number of spectral degrees of freedom (DoF), can hence be estimate as $N_f = \Delta f/\Delta f_{\text{corr}}$. Similarly, placing antennas at two positions separated by at least Δl_{corr} would constitute two spatial DoF.

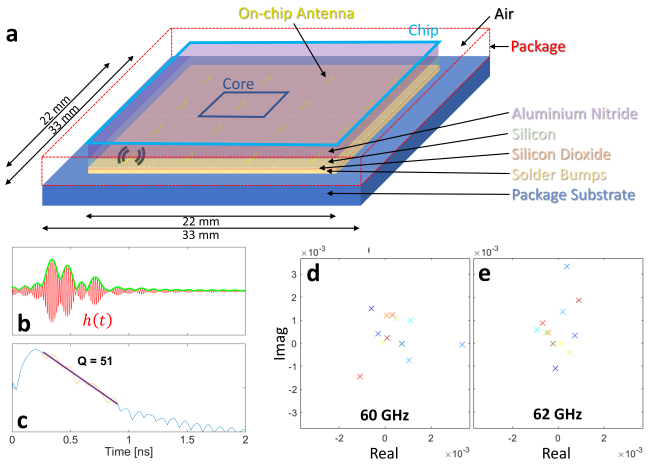

Figure 1: On-chip propagation environment. a, Chip structure (see text for details). b, Example of an impulse response $h(t)$ for a 10 GHz bandwidth centered on 60 GHz. c, Average impulse response envelope fitted to extract the enclosure's quality factor Q. d,e, Channel coefficients at two frequencies within the considered mmW regime.

The quality factor can also be interpreted as the number of times the wave (effectively) reverberates before being attenuated. To estimate Q, we compute the impulse responses between different pairs of antennas, an example is shown in Fig. 1(b). We average their envelopes and extract the exponential decay constant μ to evaluate Q as $\pi f_0/\mu$, as shown in Fig. 1(c). For the considered chip, we find $Q \approx 51$. Even though this is lower than the quality factor of indoor environments at Wi-Fi frequencies [8] and much lower than the quality factor of reverberation chambers used for electromagnetic compatibility tests, $Q \approx 51$ nonetheless indicates a non-negligible amount of reverberation inside the enclosure. The considered electromagnetic waves are more strongly attenuated in the chip environment than the corresponding waves in indoor environments. The long coda of the impulse response may cause severe inter-symbol interference.

To get an idea of the diversity of the channel coefficients, we Fourier transform the impulse responses and plot the corresponding values for two frequencies in the complex Argand diagram in Fig. 1(d,e). Both phase and amplitude of the coefficients are apparently random and the clouds are roughly centered on the origin, suggesting that this distribution of coefficients may be well described as a random complex Gaussian variable. The two example frequencies in Fig. 1(d,e) are separated by 2 GHz, which is more than the spectral correlation length $\Delta f_{\text{corr}} \approx 1.5$ GHz. Indeed, the channel coefficients at these two frequencies appear to be completely uncorrelated, as expected.

On an abstract level, WNoC propagation environments have two advantageous properties compared to indoor environments. First, as mentioned previously, they are *static* [2, 24]. Thanks to the absence of environmental perturbations, any necessary optimizations of the meta-atom configurations can be prepared off-line in a calibration phase. Specifically, the costly need for constantly re-evaluating the channel state information (CSI) in indoor environments is absent in a WNoC. Second, the environment is completely *sealed* from the outside. There are hence no spectrum allotment concerns in choosing a part of the spectrum for operation, nor any issues with interference from outside signals entering the WNoC environment.

3 PROGRAMMABLE META-ATOM DESIGN

The role of the programmable meta-atoms is to alter the scattering properties of an already non-trivial scattering enclosure. In contrast to free-space applications of programmable metasurfaces [6], in our use case the details of the electromagnetic responses of the different meta-atom states are therefore secondary as long as they are clearly distinct. Consequently, our proposal is of quite general nature and can be implemented with programmable meta-atoms based on a wide range of tuning mechanisms. The recent literature contains a variety of designs for 1-bit or multi-bit reflection-programmable meta-atoms operating at lower frequencies, typically between 2 GHz and 20 GHz [6, 18, 22, 31, 33]. In many use-case scenarios inside complex scattering environments, the cost and complexity of the necessary bias circuitry to enable continuous tuning of the meta-atom's electromagnetic response outweighs the additional gains in control over the field, such that often 1-bit programmable metasurfaces are used.

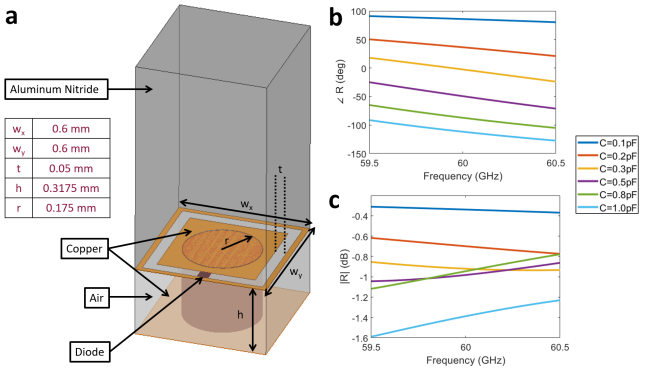

Figure 2: Programmable meta-atom design for operation at 60 GHz in the on-chip environment. a, Design of the programmable meta-atom. The inset indicates the labelled dimensions. b, Phase of reflected wave for different capacitance values of the varactor diode. c, Amplitude of reflected wave for different capacitance values of the varactor diode.

To illustrate our concept, we consider a reflection-programmable meta-atom based on a mushroom structure similar to the one in Ref. [33]. To transpose this design to the WNoC use case, we need to (i) adjust the working frequency to the 60 GHz regime, and (ii) account for the fact that the meta-atoms are immersed in AlN with a refractive index of $n = 2.9$ rather than in air as for an indoor environment. The deposition of copper on AlN has been reported in Ref. [30] and appears hence feasible. Our meta-atom design, sketched in Fig. 2(a), differs from the usual mushroom structure in that the mushroom is filled with air and the varactor diode is placed inside the mushroom. The former helps to limit the meta-atom's capacitance which is already quite high due to the high dielectric constant of the AlN layer. Otherwise, very high capacitance values for the varactor diode would be necessary to impact the resonance.

We test the performance of our design in a single-mode waveguide: in Fig. 2(b,c) we plot phase and amplitude of the wave reflected off the meta-atom for different values of the varactor diode's capacitance. Around the targeted working frequency of 60 GHz, the range of accessible phase values exceeds 180°. The reflected wave is only slightly attenuated due to its interaction with the meta-atom. Moreover, further simulation results (not shown) suggest that the impact of the meta-atom on the reflected wave is sufficiently broadband to effectively manipulate frequencies within at least a 6 GHz interval. A further possibility to enhance the bandwidth of operation consists in using different types of meta-atoms that efficiently modulate frequencies within different sub-bands of the targeted overall bandwidth. Our meta-atom design is easily adjusted to shift its central operating frequency by a few GHz. Operating at much higher frequencies, however, would require using a different switchable component (e.g. a liquid crystal).

4 OUTLOOK

In the previous sections, we have prepared the ground for the dynamic programming of on-chip wireless channels. We now discuss

a few use cases for programmable on-chip propagation environment. Thanks to the field-programmable nature of the meta-atoms, it will be feasible to straightforwardly switch between different use cases depending on traffic needs. A given use case can also be adapted dynamically to traffic needs; for instance, if distinct pairs of far-apart cores need to communicate one after the other, the metasurface-programmable on-chip propagation environment can adapt to these needs and optimize different links in a sequential manner.

4.1 Single-Channel Scenarios

We begin by considering a single-channel scenario linking, for instance, two far-apart cores on the same chip.

4.1.1 Monochromatic Channel Shaping. A first possibility here is to improve the received signal strength at the receive end, analogous to the experimental work presented in Ref. [14] for operation at 2.5 GHz in a meter-sized chaotic cavity. Inside a complex scattering enclosure, an isotropic focal spot around the receiver with a size on the order of half the wavelength is expected. The wavelength depends on the medium's refractive index n: $\lambda = \lambda_0/n$. In silicon and aluminium nitride, this yields a focal spot size of 0.7 mm and 0.9 mm, respectively. Such a focal spot would thus be restricted to an area significantly smaller than one specific core, as desired. In the spectral domain, the enhancement would affect frequencies within an interval $\Delta f_{\text{corr}} \approx 1.5$ GHz around the central operating frequency. If the bandwidth over which the energy is effectively focused is desired to be larger than Δf_{corr}, the problem becomes a multi-channel scenario since two or more independent frequencies are considered. Multi-channel scenarios are addressed in Section 4.2.1 in more detail.

To quantify an estimate of the expected achievable enhancement of the received signal strength, we consider the following toy model. The transmission between two wireless nodes in a complex scattering enclosure may be decomposed into the contribution of N different cavity modes that overlap at the working frequency due to their finite linewidth [14]. Given the chaotic nature of the geometry, this amounts to modelling the transmission as a random walk of N steps in the Argand diagram as sketched in Fig. 3. The expected value of the distance from the origin of this walk, the incoherent sum of N steps, is $\sqrt{N}$. By tuning the scattering properties of the enclosure with the programmable metasurface, we gain effectively (not literally) control over p modes [14]. The resulting distance from the origin, assuming $p < N$, is then the coherent sum of p steps and the incoherent sum of $N - p$ steps, yielding an amplitude enhancement of $\eta \approx \left(p + \sqrt{N-p}\right)/\sqrt{N}$ [14].

Having outlined the toy model, we now estimate N and p in order to quantify the expected achievable enhancement η. To quantify an upper bound p_{max} on p, we divide the chip package footprint's surface area of 33 mm×33 mm into half-wavelength squares, taking into account that for the area covering the chip the medium is not vacuum/air ($\lambda_0 = 5$ mm) but AlN ($\lambda = 1.71$ mm). Thereby, we find $p_{max} = 763$. To evaluate N, we use Weyl's law [14, 37]: $N \approx 8\pi(V/\lambda^3)/Q$, where V denotes the volume of the enclosure. Accounting once again for the presence of materials with different refractive indices inside the enclosure, we find $N \approx 81$. It should hence be feasible to achieve $p = N$ which would correspond to $\eta \approx \sqrt{N} = 9$. Such a significant enhancement can be expected to be able to counteract the strong path loss in the considered propagation environment.

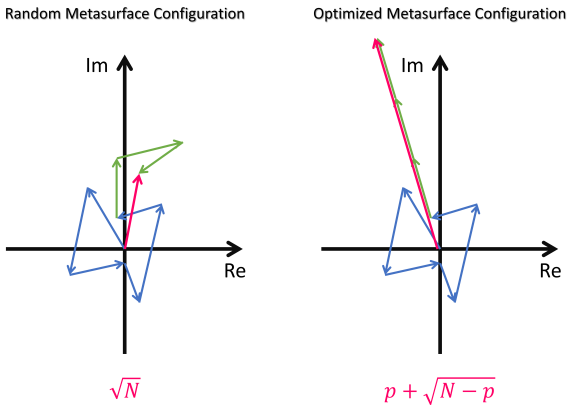

Figure 3: Model of spatial focusing in the case of $p < N$. The transmission between two wireless nodes can be decomposed into the sum of N modal contributions, represented as phasors in the Argand diagram, of which p can then be aligned coherently by optimizing the metasurface configuration.

4.1.2 Spatiotemporal Channel Shaping. Although the meta-atoms' tunability is purely of spatial nature (excluding the possibility of rapid temporal modulations of the meta-atom configurations on the order of a MHz [41]), they allow us to focus waves on the receiver not only in space but simultaneously in time. This surprising ability, evidenced experimentally in Ref. [11] in the 2.5 GHz regime, builds on the fact that complex propagation environments completely scramble spatial and temporal degrees of freedom [20]. Inter-symbol interference (ISI) arises because the received signal is the convolution of the transmitted signal pulses (assuming simple on/off keying) with the environment's impulse response which has a long coda due to multiple reverberations (see Fig. 1(b) and the left illustration in Fig. 4). The temporal length of the coda can be linked to the spectral correlation length: $\tau \approx 1/\Delta f_{\text{corr}}$. Spatiotemporal focusing offers a way to reduce ISI by essentially tailoring the impulse response between two specific wireless nodes such that most energy arrives at a specific time t_0, as illustrated on the right hand side of Fig. 4. The temporal width Δt of the optimized impulse response was found in Ref. [11] to correspond to that of the emitted pulse, irrespective of Q and hence τ. This holds as long as all frequencies contained within the emitted pulse are efficiently modulated by the meta-atoms. Spatiotemporal channel shaping therefore holds the promise of achieving a modulation rate (assuming a low-index modulation like on/off keying) that is only limited by the utilized bandwidth, but not by ISI due to multipath effects – despite operating in a complex reverberant environment. Ref. [11] showed that the achievable enhancement of the instantaneous signal in spatiotemporal focusing is independent of the amount of attenuation in the scattering enclosure; in contrast, the enhancement of deposited energy (a purely spatial effect ignoring

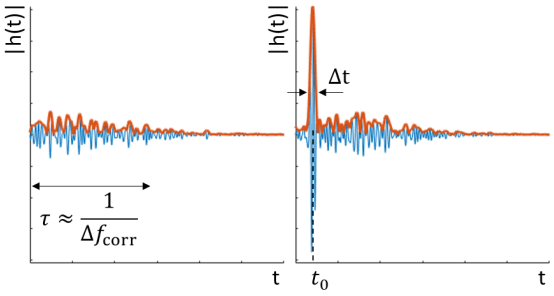

Figure 4: Illustration of spatiotemporal single-channel optimization. Left: illustration of an unoptimized impulse response. Right: illustration of an impulse response focused at t_0.

any coherent temporal effects) is larger if Q is lower. In other words, when few uncorrelated frequencies are involved in the problem, spatiotemporal focusing tends to mainly focus waves spatially as in monochromatic spatial focusing.

4.2 Multi-Channel Scenarios

Having discussed two scenarios for single-channel tailoring, we now move on to considering multi-channel scenarios.

4.2.1 Multiple independent single-channel links. Simultaneously enhancing multiple independent single-channel links (by spatial or spatiotemporal focusing as discussed in the previous section) is feasible, but of course at the cost of a lower enhancement per link. The fixed amount of control over the wave field has to be shared by multiple channels. For instance, an experimental study demonstrated that the achievable spatial-focusing intensity is inversely proportional to the number of independent channels [12]. Although Ref. [12] considered multiple spatial channels at the same frequency, analogous results are expected for multiple spectral channels between the same pair of wireless nodes [3].

4.2.2 Multiple-input multiple-output channels. A conceptually more interesting multi-channel scenario is that of multiple channels linking one transmitter with one receiver, often referred to as "multiple-input multiple-output" (MIMO) system. While the previous scenarios seek to leverage the programmability to counteract the consequences of the propagation environment's complexity, MIMO systems can actually harness this complexity and outperform their free-space counterpart [26, 32]. Shannon's generalized law,

$$C(\mathbf{H},\rho) = \log_2\left[\det\left(\mathbf{I}+\frac{\rho}{m}\mathbf{H}\mathbf{H}^\dagger\right)\right] = \sum_i \log_2\left[1+\frac{\rho}{m}\sigma_i^2\right], \quad (1)$$

reveals that in a MIMO use case, the channel diversity (represented by the singular value decomposition of the $m \times m$ monochromatic channel matrix $\mathbf{H}$) plays a crucial role besides the signal-to-noise ratio ρ. While in free space only one singular value may be significant, in a randomly scattering medium the singular value spectrum declines only slowly. A useful metric to quantify the channel diversity is the effective rank [29]: $R_{\text{eff}} = \exp\left[-\sum_i \sigma_i' \ln(\sigma_i')\right]$, where $\sigma_i' = \sigma_i / \sum_i \sigma_i$. For instance, a 5×5 channel matrix with random entries (Rayleigh model) yields $R_{\text{eff}} = 4.1$. By using a random configuration of the programmable metasurface, the on-chip propagation environment can be expected to act like a random scattering medium [16].

However, the programmability helps to push these advantages even further, beyond those attainable in purely random media, all the way to $R_{\text{eff}} = m$, if carefully optimized rather than random configurations are used [7, 8]. While improvements of ρ become inefficient as the number of channels increases [12], tweaking the channels to improve their distinguishability requires much less control over the environment's scattering properties [8]. In the given chip use-case scenario, considering a macro-receiver consisting of multiple cores, each with one antenna, would only be reasonable if those receiving cores were in close proximity so that they could cooperate regarding the decoding of the received information. We therefore consider the case of core-to-core communication with multiple antennas per core more interesting. The latter has to date largely been discarded due to space constraints but can be realized with vertical through-silicon-via monopole antennas [27]. Given the wavelength in silicon of 0.7 mm, the number of spatial DoF per core is $((22/4)\text{ mm})^2/((0.7\text{ mm})^2) \approx 61$. In other words, the upper bound on the number of independent vertical monopole antennas per core area is 61 and hence largely above what would be needed for a MIMO link. Note that this value is so high thanks to the speckle-like nature of the field with $\Delta l_{\text{corr}} \approx \lambda/2$. Monopole antennas lack directivity but the latter is only of limited utility in reverberant media anyway; Ref. [8] also considered two arrays of monopole antennas to study the tuning of $\mathbf{H}$ at the indoor scale. The potentially significant improvements of the capacity come, however, at the cost of having to decode the received data. This operation can be accomplished with simple tools, such as Tikhonov regularization [34]. Moreover, we recall that CSI is static in a WNoC; CSI can hence be evaluated off-line and the decoders can be prepared off-line, too.

5 CONCLUSION

To summarize, this manuscript outlines our first steps toward endowing on-chip wireless propagation environments with programmability by equipping them with programmable metasurfaces akin to current trends in indoor wireless communication. We characterized a representative on-chip propagation environment, proposed a possible design of a programmable meta-atom operating at 60 GHz inside the chip package, and discussed various use cases of the programmable scattering properties of the propagation environment. In future work, we will numerically study the proposed ideas for channel tuning in full-wave simulations. We faithfully expect that the introduced perspective for in-situ programmable on-chip wireless communication channels will open up unprecedented possibilities for multiprocessor interconnection on modern chips.

ACKNOWLEDGMENTS

S.A. acknowledges support from the European Commission through the H2020 FET-OPEN program under grants No. 736876 and No. 863337.

REFERENCES

[1] Sergi Abadal, Chong Han, and Josep Miquel Jornet. 2019. Wave propagation and channel modeling in chip-scale wireless communications: A survey from millimeter-wave to terahertz and optics. *IEEE Access* 8 (2019), 278–293.

[2] Sergi Abadal, Albert Mestres, Josep Torrellas, Eduard Alarcón, and Albert Cabellos-Aparicio. 2018. Medium access control in wireless network-on-chip: A context analysis. *IEEE Commun. Mag.* 56, 6 (2018), 172–178.

[3] Daria Andreoli, Giorgio Volpe, Sébastien Popoff, Ori Katz, Samuel Grésillon, and Sylvain Gigan. 2015. Deterministic control of broadband light through a multiply scattering medium via the multispectral transmission matrix. *Sci. Rep.* 5 (2015), 10347.

[4] Davide Bertozzi, Giorgos Dimitrakopoulos, José Flich, and Sören Sonntag. 2015. The fast evolving landscape of on-chip communication. *Des. Autom. Embed. Syst.* 19, 1-2 (2015), 59–76.

[5] M Frank Chang, Vwani P Roychowdhury, Liyang Zhang, Hyunchol Shin, and Yongxi Qian. 2001. RF/wireless interconnect for inter-and intra-chip communications. *Proc. IEEE* 89, 4 (2001), 456–466.

[6] Tie Jun Cui, Mei Qing Qi, Xiang Wan, Jie Zhao, and Qiang Cheng. 2014. Coding metamaterials, digital metamaterials and programmable metamaterials. *Light Sci. Appl.* 3, 10 (2014), e218–e218.

[7] Philipp del Hougne, Matthieu Davy, and Ulrich Kuhl. 2020. Optimal multiplexing of spatially encoded information across custom-tailored configurations of a metasurface-tunable chaotic cavity. *Phys. Rev. Applied* 13, 4 (2020), 041004.

[8] Philipp del Hougne, Mathias Fink, and Geoffroy Lerosey. 2019. Optimally diverse communication channels in disordered environments with tuned randomness. *Nat. Electron.* 2, 1 (2019), 36–41.

[9] Philipp del Hougne, Mohammadreza F Imani, Aaron V Diebold, Roarke Horstmeyer, and David R Smith. 2020. Learned integrated sensing pipeline: Reconfigurable metasurface transceivers as trainable physical layer in an artificial neural network. *Adv. Sci.* 7, 3 (2020), 1901913.

[10] Philipp del Hougne, Mohammadreza F Imani, Mathias Fink, David R Smith, and Geoffroy Lerosey. 2018. Precise localization of multiple noncooperative objects in a disordered cavity by wave front shaping. *Phys. Rev. Lett.* 121, 6 (2018), 063901.

[11] Philipp del Hougne, Fabrice Lemoult, Mathias Fink, and Geoffroy Lerosey. 2016. Spatiotemporal wave front shaping in a microwave cavity. *Phys. Rev. Lett.* 117, 13 (2016), 134302.

[12] Philipp del Hougne, Boshra Rajaei, Laurent Daudet, and Geoffroy Lerosey. 2016. Intensity-only measurement of partially uncontrollable transmission matrix: demonstration with wave-field shaping in a microwave cavity. *Opt. Express* 24, 16 (2016), 18631–18641.

[13] Marco Di Renzo, Merouane Debbah, Dinh-Thuy Phan-Huy, Alessio Zappone, Mohamed-Slim Alouini, Chau Yuen, Vincenzo Sciancalepore, George C Alexandropoulos, Jakob Hoydis, Haris Gacanin, et al. 2019. Smart radio environments empowered by reconfigurable AI meta-surfaces: An idea whose time has come. *J. Wirel. Commun. Netw.* 2019, 1 (2019), 1–20.

[14] Matthieu Dupré, Philipp del Hougne, Mathias Fink, Fabrice Lemoult, and Geoffroy Lerosey. 2015. Wave-field shaping in cavities: Waves trapped in a box with controllable boundaries. *Phys. Rev. Lett.* 115, 1 (2015), 017701.

[15] Mohammadreza F. Imani, David R Smith, and Philipp del Hougne. 2020. Perfect Absorption in a Disordered Medium with Programmable Meta-Atom Inclusions. *Adv. Funct. Mater.* TBA (2020), 2005310.

[16] Jean-Baptiste Gros, Philipp del Hougne, and Geoffroy Lerosey. 2020. Tuning a regular cavity to wave chaos with metasurface-reconfigurable walls. *Phys. Rev. A* 101, 6 (2020), 061801.

[17] Felix Gutierrez, Shatam Agarwal, Kristen Parrish, and Theodore S Rappaport. 2009. On-chip integrated antenna structures in CMOS for 60 GHz WPAN systems. *IEEE J. Sel. Areas Commun.* 27, 8 (2009), 1367–1378.

[18] Nadège Kaina, Matthieu Dupré, Mathias Fink, and Geoffroy Lerosey. 2014. Hybridized resonances to design tunable binary phase metasurface unit cells. *Opt. Express* 22, 16 (2014), 18881–18888.

[19] Kihong Kim, Brian A Floyd, Jesal L Mehta, Hyun Yoon, Chih-Ming Hung, Dan Bravo, Timothy O Dickson, Xiaoling Guo, Ran Li, Narasimhan Trichy, et al. 2005. On-chip antennas in silicon ICs and their application. *IEEE Trans. Electron Devices* 52, 7 (2005), 1312–1323.

[20] Fabrice Lemoult, Geoffroy Lerosey, Julien de Rosny, and Mathias Fink. 2009. Manipulating spatiotemporal degrees of freedom of waves in random media. *Phys. Rev. Lett.* 103, 17 (2009), 173902.

[21] Hao-Yang Li, Han-Ting Zhao, Meng-Lin Wei, Heng-Xin Ruan, Ya Shuang, Tie Jun Cui, Philipp del Hougne, and Lianlin Li. 2020. Intelligent Electromagnetic Sensing with Learnable Data Acquisition and Processing. *Patterns* 1, 1 (2020), 100006.

[22] Fu Liu, Odysseas Tsilipakos, Alexandros Pitilakis, Anna C Tasolamprou, Mohammad Sajjad Mirmoosa, Nikolaos V Kantartzis, Do-Hoon Kwon, Maria Kafesaki, Costas M Soukoulis, and Sergei A Tretyakov. 2019. Intelligent metasurfaces with continuously tunable local surface impedance for multiple reconfigurable functions. *Phys. Rev. Applied* 11, 4 (2019), 044024.

[23] David W Matolak, Savas Kaya, and Avinash Kodi. 2013. Channel modeling for wireless networks-on-chips. *IEEE Commun. Mag.* 51, 6 (2013), 180–186.

[24] David W Matolak, Avinash Kodi, Savas Kaya, Dominic Ditomaso, Soumyasanta Laha, and William Rayess. 2012. Wireless networks-on-chips: architecture, wireless channel, and devices. *IEEE Wirel. Commun.* 19, 5 (2012), 58–65.

[25] David AB Miller. 2009. Device requirements for optical interconnects to silicon chips. *Proc. IEEE* 97, 7 (2009), 1166–1185.

[26] Aris L Moustakas, Harold U Baranger, Leon Balents, Anirvan M Sengupta, and Steven H Simon. 2000. Communication through a diffusive medium: Coherence and capacity. *Science* 287, 5451 (2000), 287–290.

[27] Vasil Pano, Ibrahim Tekin, Isikcan Yilmaz, Yuqiao Liu, Kapil R Dandekar, and Baris Taskin. 2020. TSV Antennas for Multi-Band Wireless Communication. *IEEE Trans. Emerg. Sel. Topics Circuits Syst.* 10, 1 (2020), 100–113.

[28] William Rayess, David W Matolak, Savas Kaya, and Avinash Karanth Kodi. 2017. Antennas and channel characteristics for wireless networks on chips. *Wirel. Pers. Commun.* 95, 4 (2017), 5039–5056.

[29] Olivier Roy and Martin Vetterli. 2007. The effective rank: A measure of effective dimensionality. In *15th European Signal Processing Conference*. IEEE, 606–610.

[30] Shao-Ping Shen and Wei-Ping Dow. 2014. Adhesion enhancement of a plated copper layer on an AlN substrate using a chemical grafting process at room temperature. *J. Electrochem. Soc.* 161, 10 (2014), D579.

[31] Daniel F Sievenpiper, James H Schaffner, H Jae Song, Robert Y Loo, and Gregory Tangonan. 2003. Two-dimensional beam steering using an electrically tunable impedance surface. *IEEE Trans. Antennas Propag.* 51, 10 (2003), 2713–2722.

[32] Steven H Simon, Aris L Moustakas, Marin Stoytchev, and Hugo Safar. 2001. Communication in a disordered world. *Phys. Today* 54, 9 (2001).

[33] Timothy Sleasman, Mohammadreza F Imani, Jonah N Gollub, and David R Smith. 2016. Microwave imaging using a disordered cavity with a dynamically tunable impedance surface. *Phys. Rev. Applied* 6, 5 (2016), 054019.

[34] Andrey Nikolayevich Tikhonov. 1963. Solution of incorrectly formulated problems and the regularization method. *Soviet Math. Dokl.* 4 (1963), 1035.

[35] Xavier Timoneda, Sergi Abadal, Antonio Franques, Dionysios Manessis, Jin Zhou, Josep Torrellas, Eduard Alarcón, and Albert Cabellos-Aparicio. 2020. Engineer the Channel and Adapt to it: Enabling Wireless Intra-Chip Communication. *IEEE Trans. Commun.* 68, 5 (2020), 3247–3258.

[36] David Wentzlaff, Patrick Griffin, Henry Hoffmann, Liewei Bao, Bruce Edwards, Carl Ramey, Matthew Mattina, Chyi-Chang Miao, John F Brown III, and Anant Agarwal. 2007. On-chip interconnection architecture of the tile processor. *IEEE Micro* 27, 5 (2007), 15–31.

[37] Hermann Weyl. 1911. Über die asymptotische Verteilung der Eigenwerte. *Nachrichten von der Gesellschaft der Wissenschaften zu Göttingen, Mathematisch-Physikalische Klasse* 1911 (1911), 110–117.

[38] Junqiang Wu and Hao Xin. 2017. Novel 3D-printing enabled antenna design for future wireless intra-chip interconnect. In *2017 IEEE International Symposium on Antennas and Propagation & USNC/URSI National Radio Science Meeting*. IEEE, 1237–1238.

[39] Xinmin Yu, Joe Baylon, Paul Wettin, Deukhyoun Heo, Partha Pratim Pande, and Shahriar Mirabbasi. 2014. Architecture and design of multichannel millimeter-wave wireless NoC. *IEEE Des. Test* 31, 6 (2014), 19–28.

[40] Xinmin Yu, Suman Prasad Sah, Hooman Rashtian, Shahriar Mirabbasi, Partha Pratim Pande, and Deukhyoun Heo. 2014. A 1.2-pJ/bit 16-Gb/s 60-GHz OOK transmitter in 65-nm CMOS for wireless network-on-chip. *IEEE Trans. Microw. Theory Tech.* 62, 10 (2014), 2357–2369.

[41] Lei Zhang, Xiao Qing Chen, Rui Wen Shao, Jun Yan Dai, Qiang Cheng, Giuseppe Castaldi, Vincenzo Galdi, and Tie Jun Cui. 2019. Breaking reciprocity with space-time-coding digital metasurfaces. *Adv. Mater.* 31, 41 (2019), 1904069.

[42] Hanting Zhao, Ya Shuang, Menglin Wei, Tie Jun Cui, Philipp del Hougne, and Lianlin Li. 2020. Metasurface-assisted massive backscatter wireless communication with commodity Wi-Fi signals. *Nat. Commun.* 11, 1 (2020), 1–10.